ESA Climate Change Initiative “Plus” (CCI+)

End-to-End ECV Uncertainty Budget (E3UB) Version 4.0

-

For the RemoTeC XCH4 GOSAT-2 SRON Proxy Product

(CH4_GO2_SRPR) Version 2.0.2

for the Essential Climate Variable (ECV)

Greenhouse Gases (GHG)

Written by:

GHG-CCI+ project team

Lead author:

Andrew Gerald Barr

(SRON Netherlands Institute for Space Research, Leiden, The Netherlands)

Co-authors:

Tobias Borsdorff, Jochen Landgraf

(SRON Netherlands Institute for Space Research, Leiden, The Netherlands)

Change log

Version Nr.	Date	Status	Reason for change
Version 1.0	27 Oct. 2020	Draft	New document
Version 1.1	4. Jan. 2021	As submitted	- Definition uncertainty ratio - Update format - Remove typos
Version 1.1	4. Feb. 2021	As submitted	- Update after ESA reviews - Remove typos
Version 2.0	04. Nov. 2021	As submitted	- Updated to version 2.0.0
Version 3.0	27. Jan. 2022	As submitted	- Updated doc to version 3.0
Version 4.0	18. Apr. 2023	As submitted	- Updated doc to version 4.0 - Quality filtering via random forest model prediction

Table of Contents

Executive summary

This report summarizes the performance of the RemoTeC GOSAT-2 SRPR XCH_4 retrieval. In general, we find very good agreement with TCCON and GOSAT data for the two modes (land and ocean). The mean bias (global offset) is -0.12 ppb with a single measurement precision of 16.56 ppb. The spatial accuracy (standard deviation site biases) is 5.90 ppb, however this is reduced to 4.36 ppb when excluding the coastal TCCON stations Izana and Rikubetsu which have particulary high bias, potentially related to the bias correction. The mean standard deviation of around 15.38 ppb is observed for most TCCON stations. Based on comparison with TCCON we scale the retrieved statistical error by a factor 1.93 for land mode and 1.66 for glint mode to obtain a representative random error. This corresponds to an uncertainty ratio of 0.81 for land mode and 0.81 glint mode.

Estimates of achieved data quality: CH4_GO2_SRPR					
Sensor	**Algorithm**	**Single measurement precision (1-sigma) in [ppb]**	**Mean bias (global offset) [ppb]**	**Spatial Accuracy: Relative systematic error [ppb]**	**Uncertainty ratio (scaling)**
TANSO-FTS-2 on GOSAT-2	RemoTeC	16.56	-0.12	5.90	0.81

Table 1: An overview of the achieved data quality for the XCH_4 SRPR product.

1 Introduction

1.1 Purpose of document

This E3UB provides an overview of random and systematic errors affecting the SRON SRPR XCH_4 retrieval submitted for the ESA GHG-CCI+ Climate Research Data Package 8. Application of confidence limits to the retrieval is required to translate remotely sensed data presented here into modelled estimations with a known degree of confidence, allowing detection of climate change impacts additional to the natural variability of greenhouse gases. In particular, the GHG-CCI+ User Requirements have placed strict measurement accuracy and precision requirements on the participating GHG retrievals, allowing identification of minute changes in magnitude and sign of XCH_4 concentration change (Buchwitz et al., 2011; 2014).

1.2 Intended audience

This document is intended for users in the modelling community applying the SRPR XCH_4 product for CO_2 inversions, as well as remote sensing experts interested in atmospheric soundings of XCH_4. In both cases the work presented here will give the user a more thorough understanding of error implicit in this GHG-CCI+ product.

1.3 Error term definitions

Error terms used in this report are defined to maintain consistency with other CCI+ user group error terms recommended at the 2014 CCI co-location meeting. Following the descriptions of Wagner et al. (2012):

Error	Difference between measured values and reality (residual of a measurement's accuracy).
Uncertainty	Degree of confidence in the range of a measured value's truth (standard deviation).
Absolute accuracy	Proximity of remotely sensed measurement to in-situ measurement, assuming the in-situ measurement is able to provide a best estimate of observed quantity. Absolute accuracy reflects the best effort of the remote sensing system at reproducing the real world value by incorporating all random and systematic errors affecting the retrieval.
Relative accuracy	Ratio between the instrument's calibration standard (the best possible measurement the instrument is able to make) against the instrument characteristics at the time of measurement.

Precision	Repeatability of a measurement.
Sensitivity	Change of measurement due to instrumental and algorithmic response to physical or simulated input parameters.

2 Error sources

The majority of error is added to measurements from sources grouped into two themes – scattering of radiation into and out of the sensed light path by poorly quantified aerosol loading, cloud, surface reflectivity and meteorological parameters (temperature, pressure and humidity); and instrumental uncertainties (e.g. cross section and solar model inaccuracy, system noise and measurement resolution of instrument components; Connor et al., 2008, Boesch et al., 2011). In addition to single measurement error, issues of correlation lengths are introduced when the retrievals are used for subsequent generation of level 3 products (Buchwitz et al., 2014; Chevalier et al., 2014). The aforementioned errors can be further grouped into systematic – those which remain stable across measurement series; and random error components – noise in the system induced by unexpected and / or unaccounted for stimuli.

2.1 Systematic

Systematic retrieval errors include algorithmic effects such as inaccuracy in the solar and radiative transfer models, which will not change with the duration of the satellite's sensing. The same applies to restrictions in instrument calibration accuracy, for instance modelling of the instrument line shape, which remains fixed following launch (although is modifiable when enough information on ILS degradation is built up). Viewing geometry also affects retrievals in a regular fashion by modifying the light path of sensed radiation as a function of the instrument and Sun's position, however interplay between increased path lengths and random error components such as aerosol optical depth add complications to issue of measurement geometry. A-priori error added to XCO_2 and XCH_4 measurements occurs when the retrieval receives inaccurate input data from models and databases of surface reflectivity, surface pressure, vertical pressure grids, humidity profiles and a-priori CO_2 and CH_4 profiles.

2.2 Random

Random errors are introduced to observations at the sensing stage of a measurement by detector noise, although to a certain extent this error parameter can be estimated as a function of detector component signal to noise ratios during instrument calibration. Far more significantly, atmospheric parameters are able to have major effects on sounding measurements by scattering light in and out of the sensed column. Errors due to unknown aerosol parameters are particularly pronounced where the scattering and absorption effects of suspended particulate matter are poorly modelled, as they inevitably will be when accounting for a tiny subset of all aerosol sizes, morphology and composition. Scattering due to high, optically thin clouds that are not screened from observation record present similar problems.

3 Methodology

3.1 SRON SRPR

The CH4_GO2_SRPR product is retrieved from GOSAT-2 TANSO-FTS SWIR spectra using the RemoTeC algorithm that has been jointly developed at SRON and KIT (Butz et al., 2009; Butz et al., 2010; Butz et al., 2011, Schepers et al 2012) which is also used used for the GOSAT retrievals. The algorithm retrieves simultaneously XCH_4 and XCO_2. For the retrieval, we analyze four spectral regions: the 0.77 µm oxygen band, two CO_2 bands at 1.61 and 2.06 µm, as well as a CH_4 band at 1.64 µm. A small difference between the GOSAT and -2 retrievals is that the GOSAT-2 retrieval uses a slightly shortened retrieval window for the O_2-A Band as described in the version 1.0 ATBD document **(**Krisna et al. 2020**)**. Within the retrieval procedure the sub-columns of CO_2 and CH_4 in different altitude layers are being retrieved. To obtain the column averaged dry air mixing ratios XCO_2 and XCH_4 the sub-columns are summed up to get the total column which is divided by the dry-air columns obtained from ECMWF model data in combination with a surface elevation data base. As the PROXY retrievals perform a non-scattering retrieval, the retrieved XCH_4 column cannot be used directly, as effects of aerosol scattering modify the light path. To correct for this, in the PROXY approach, the retrieved XCH_4 column is divided by the retrieved XCO_2 column at the 1.61 µm band and then multiplied by a XCO_2 total column obtained from the Copernicus Atmosphere Monitoring Service (CAMS). The inversion products used for XCO_2 are the official CAMS v19r1, v20r2 and v21r1 products (Chevallier et al., 2019).

The retrieved XCH_4 has been validated with ground based TCCON measurements. To further improve accuracy a bias correction has been developed based on TCCON comparisons. We use the GGG2020 release of the TCCON data. The CH4_GO2_SRPR product v2.0.2 covers the period from start of measurements (February 2019) up until the end of December 2021. More details on the technical aspects of the retrievals can be found in the version 4.0 ATBD GO2-SRPR document (Barr et al. 2023).

3.2 TCCON

The Total Carbon Column Observing Network (TCCON) is a global network of Fourier transform spectrometers built for the purpose of validating space-borne measurements of XCO_2 and XCH_4 (Wunch et al. 2015, Laughner et al. 2021). TCCON observes these gases with a precision on mole fractions of ~0.15% and ~0.2% for CO_2 and CH_4 respectively (Toon et al., 2009). Although providing highly accurate measurements, the sparseness of the TCCON sites presents a challenge for validation; offering precise GHG measurements for only a limited range of geographic and meteorological conditions.

Additional considerations should be made when validating with TCCON data for differing sensitivity of instruments between TCCON and the satellite instrument, reflected in a-priori information used for each retrieval. Removing the influence of the retrieval a-priori, and replacing with the TCCON a-priori allows for a fairer comparison between the two datasets, although slight differences in retrieval methodologies prevent a 1:1 comparison. Users of GHG-CCI+ data (particularly in the modelling community) should note that the published CCI+ products are not corrected with TCCON a-priori information (due to a-priori differences between sites), and so will find slightly worse correlations between satellite retrieved GHGs and TCCON values in their own comparisons.

TCCON data used for error assessments come from the GGG2020 collection (available from https://tccondata.org/).

3.2.1 Colocation

To assess the quality of SRPR retrieval XCH_4 observations against rigorously validated ground based TCCON values, SRPR soundings are matched to TCCON observations spatially and temporally. The process of matching these two data sources is referred to as co-location. Below we detail the SRON co-location techniques, whose methodology has a bearing on subsequent error statistics.

Spatial

We follow a straightforward approach by using a box ± 2.5°in latitude and longitude around every TCCON station.

Temporal

Matching SRPR soundings with TCCON sites for time is a comparatively simple operation, selecting only those TCCON values whose observation time falls within ±2 hours of each GOSAT-2 sounding time. The average is taken of all TCCON points fitting the above criteria for each SRPR sounding to provide the TCCON value against which to compare.

3.2.2 Bias Correction

From comparison with TCCON it was found that the error in XCH_4 correlates with the retrieved albedo α at 1.6 µm in band 2. Based on this correlation the following bias correction has been developed for XCH_4:

$$XCH4_{corr} = XCH4 * (a + b * \alpha) \quad (1)$$

Where we use here a = 0.9938 , b = 0.00021 for retrievals over land.

For retrievals over ocean, GOSAT-2 measures in sun-glint mode. Sun-glint mode takes advantage of specific viewing angle where the radiance of back-scattered sunlight is higher due to reflection from waves. This amplifies the albedo, allowing retrievals over ocean to be carried out, where the albedo is generally too low to retrieve accurate concentrations. We find that the error in XCH_4 correlates with the bias better for the retrieved ratio of O_2. As such we apply a similar bias correction as in equation 1 but with the O_2 ratio, r:

$$XCH4_{corr} = XCH4 * (a + b * r) \quad (2)$$

Where we take a = 0.99768 and b = -0.00641.

3.3 Comparison to GOSAT SRPR

The GOSAT SRPR retrieval (CH4_GOS_SRPR product) has been extensively validated and offers an excellent opportunity for comparison. We split the GOSAT-2 observations into land (ocean) and non-glint (land) sets and compare them separately. As both satellites observe at similar overpass times, we will co-locate the GOSAT and GOSAT-2 footprints spatially by classing them into 2°x2° boxes and temporally by matching the overpasses by day. All groupings are then averaged to create daily averaged 2°x2° values. Any GOSAT-2 grouping that does not have a corresponding match for GOSAT is discarded.

4 Error results

In this section we report on the comparison of the GOSAT-2 SRPR XCH_4 data providing validation of the data product using TCCON measurements and also colocations with GOSAT, for retrievals over both land and ocean.

4.1 Overview TCCON statistics

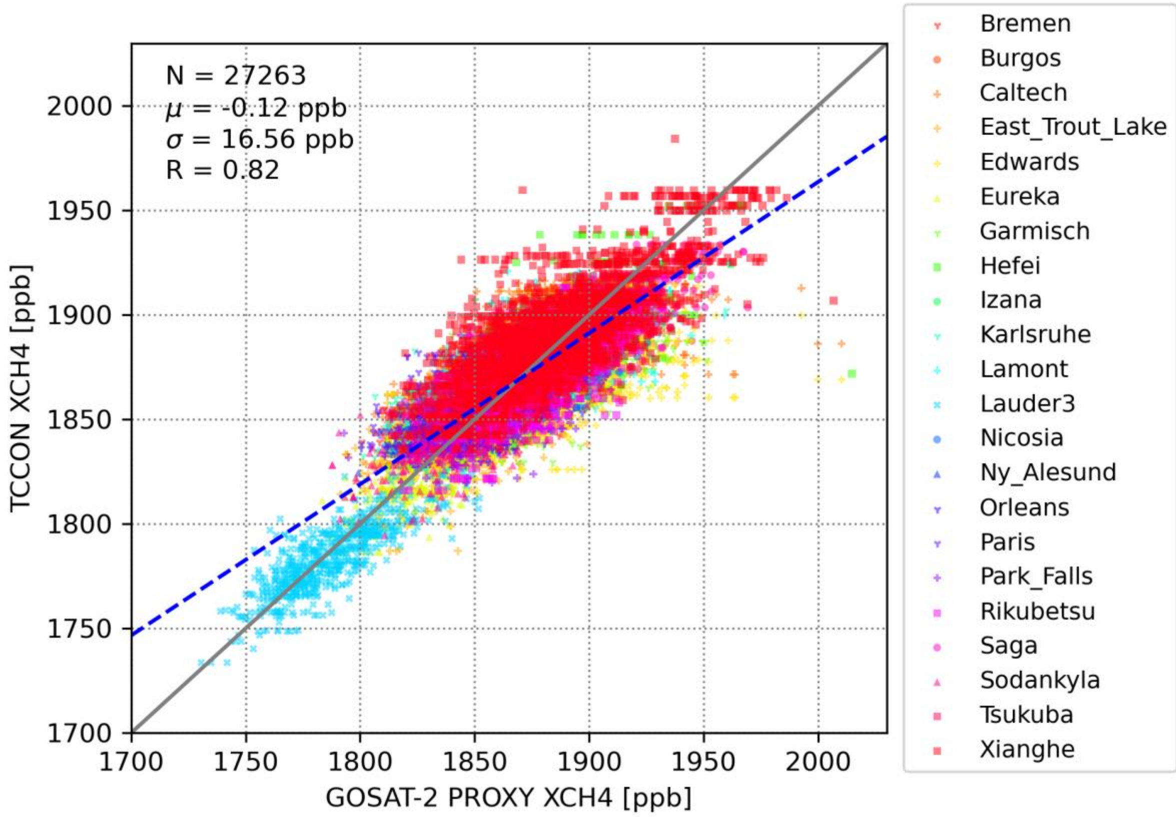

Figure 4.1 Validation of land single soundings of XCH_4 with co-located TCCON measurements at all TCCON sites for the period Feb 2019 to end Dec 2021. Numbers in the figures: μ = bias, i.e., average of the difference; σ = single measurement precision, i.e., standard deviation of the difference; N = number of co-locations; R the correlation coefficient. Stations that are along the coast and also sensitive to glint mode (ocean) measurements are indicated as circles. Those that have high latitudes in the northern and southern hemispheres are upward triangles and crosses, respectively. Stations in Asia, North America and Europe are indicated by squares, pluses and downward triangles respectively. Error bars are not shown due to the large number of data points, however they are of a similar order to those shown in Figure 4.2.

Figures 4.1 and 4.2 shows a strong correlation of the retrieved (bias-corrected) XCH_4 with the TCCON XCH_4 (r ~ 0.82 for land and 0.91 for ocean). This gives us confidence that our bias correction based on the retrieved albedo works correctly and takes out most of the bias.

Tables 4.1 and 4.2 show in detail for each station the remaining bias and standard deviation for the co-located GOSAT-2 soundings. The time-series for the sites are shown in Figure 4.3. Daily averages of XCH_4 are provided for TCCON as the variation throughout the course of one day are minimal at TCCON stations, whereas all collocated GOSAT-2 measurements are provided.

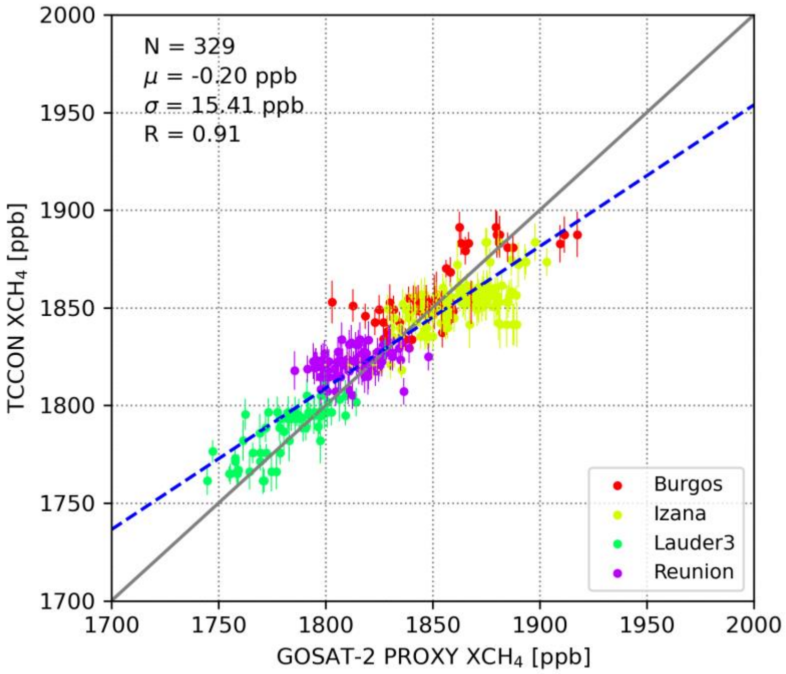

Figure 4.2 Validation of ocean single soundings of XCH_4 with co-located TCCON measurements at all TCCON sites for the period Feb 2019 to end Dec 2021. Numbers in the figures: μ = bias, i.e., average of the difference; σ = single measurement precision, i.e., standard deviation of the difference; N = number of co-locations; R the correlation coefficient. Error bars are shown on XCH_4 for GOSAT-2 as the relative error for XCH_4 from TCCON is negligible.

For land mode, the spatial accuracy (standard deviation site biases) is 5.90 ppb. The most notable outliers are Izana and Rikubetsu, with a remaining bias of 16.64 ppb and 11.04 ppb, respectively. Izana is located on an island in the Canary Islands, in Spain, therefore is one of the only stations with ocean (glint-mode) TCCON colocations. Rikubetsu is a station in Japan and is also close to Ocean. We use a different bias correction for land and ocean retrievals, and the values listed in Table 4.1 are for land retrievals only, therefore this may be the result of these high biases with stations close to the coast, however the other costal stations Burgos and Lauder have low biases with the land bias correction. If we would exclude these two stations from the calculation of the spatial accuracy, we find that this metric improves to 4.36 ppb. We note that there are only 5 colocations for Izana and hence the staistics for this station may not be reliable.

For measurements over ocean the correlation is higher, and single measurement precision ~ 1 ppb lower, than for measurements over land, however the spatial accuracy is lower by ~ 1.5 ppb. This suggests that while the glint mode retrievals are consistent, overall biases remain higher compared to land retrievals.

Table 4.1: Overview of the SRPR/RemoTeC XCH_4 validation with TCCON (after bias correction) for land retrievals.

TCCON site [Land mode]	Number of co-locations [-]	Mean difference [ppb]	Standard deviation of difference [ppb]
Bremen	250	-2.47	18.27
Burgos	463	3.29	13.37
Caltech	5423	-8.00	15.27
East_Trout_Lake	860	4.74	16.83
Edwards	6524	4.21	15.85
Eureka	132	8.44	13.32
Garmisch	631	8.96	18.86
Hefei	305	1.87	19.01
Izana	5	16.64	12.01
Karlsruhe	724	-4.75	15.44
Lamont	2535	1.27	14.17
Lauder	677	3.07	11.90

Nicosia	774	2.94	13.32
Ny_Alesund	7	-4.49	16.30
Orleans	546	-3.68	14.02
Paris	733	-5.65	14.81
Park_Falls	970	3.86	15.47
Rikubetsu	658	11.04	14.61
Saga	1603	2.38	14.79
Sodankyla	375	0.10	17.10
Tsukuba	613	-0.87	14.79
Xianghe	2455	-4.93	18.94
All observations	27263	-0.12	16.56

Table 4.2: Overview of the SRPR/RemoTeC XCH_4 validation with TCCON (after bias correction) for ocean retrievals.

TCCON site [Glint mode]	Number of co-locations [-]	Mean difference [ppb]	Standard deviation of difference [ppb]
Burgos	47	-6.12	15.50
Izana	127	10.28	13.88
Lauder	65	-4.45	9.93
Reunion	90	-8.81	11.79
All observations	329	-0.20	12.78

Table 4.3: Overview of the GOSAT-2 XCH_4 products vs TCCON co-located measurements. The mean bias μ and single measurement precision σ are calculated by taking the mean and standard deviation of the differences of all GOSAT-2 and TCCON pairs. The mean of the site means $\bar{\mu}$ and the spatial accuracy $\sigma_{\bar{\mu}}$ are calculated by taking the mean and standard deviation of the site means. The mean standard deviation $\bar{\sigma}$ and and standard deviation of the standard deviations $\sigma_{\bar{\sigma}}$ are calculated by taking the mean and the standard deviation of the site standard deviations.

	PROXY					
Variable	N	μ (ppb)	σ (ppb)	$\bar{\mu} \pm \sigma_{\bar{\mu}}$ (ppb)	$\bar{\sigma} \pm \sigma_{\bar{\sigma}}$ (ppb)	R
GOSAT2 Land	27263	-0.12	16.56	1.73 ± 5.90	15.38 ± 2.06	0.82
GOSAT-2 Ocean	329	-0.20	15.41	-2.27 ± 7.42	12.78 ± 2.10	0.91

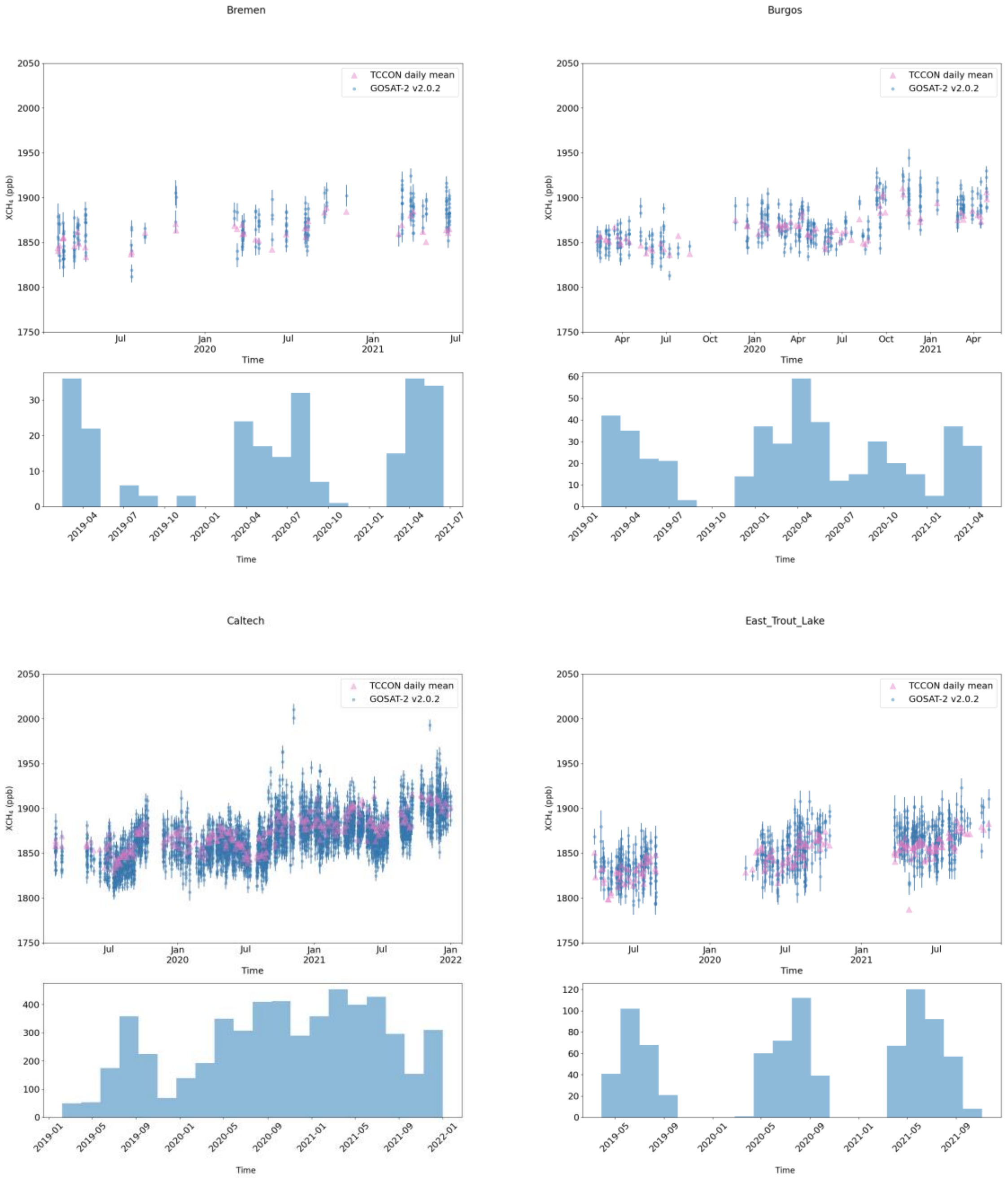

Figure 4.3 Comparison of land single soundings of XCH_4 from the proxy retrieval (blue circles) with co-located TCCON (pink triangles) measurements at all TCCON sites for the period Feb 2019 to Dec 2021. Histograms are also given for each station indicating the number of GOSAT-2 retrievals present throughout the time series.

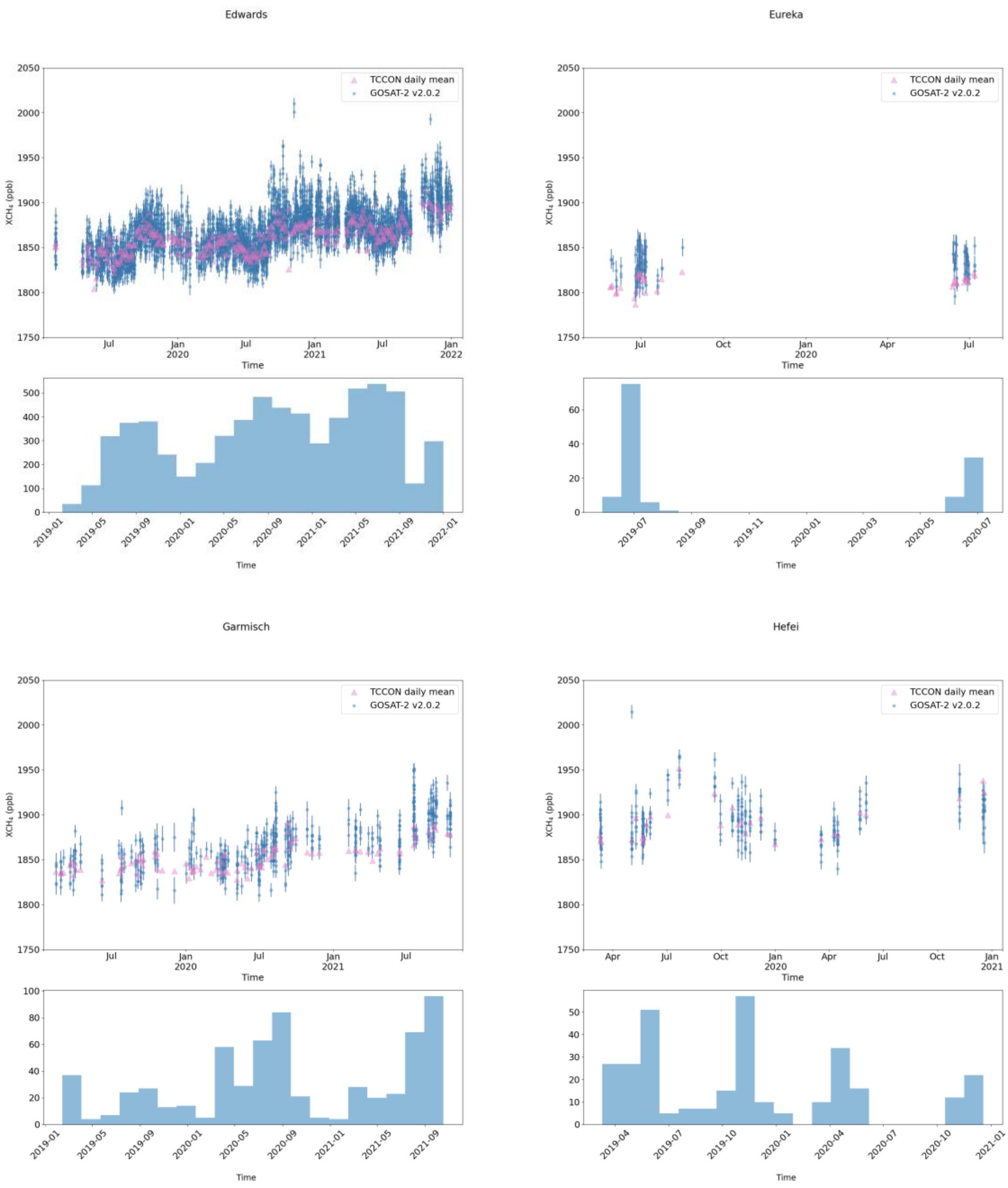

Figure 4.3 Cont.

Figure 4.3 Cont.

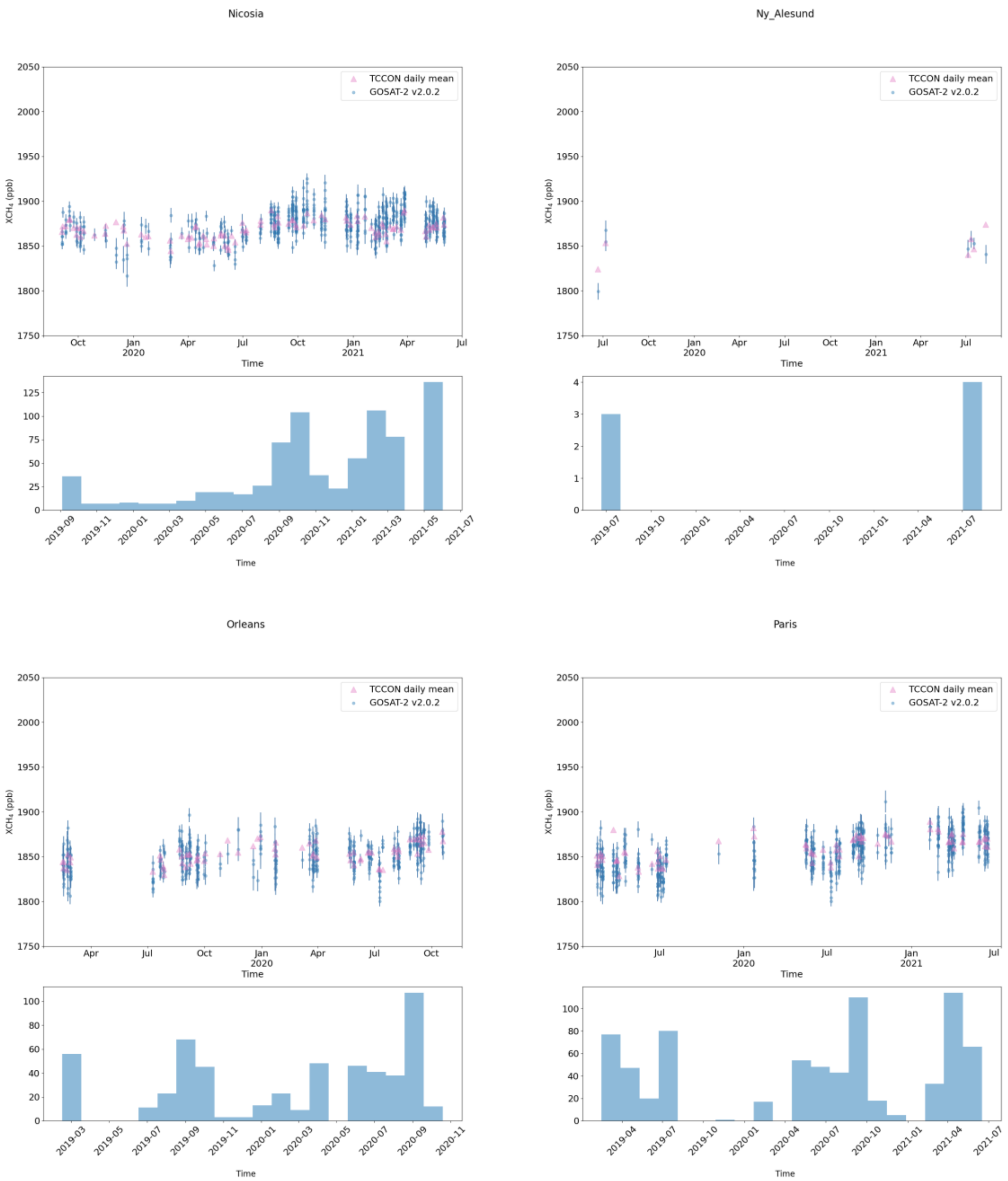

Figure 4.3 Cont.

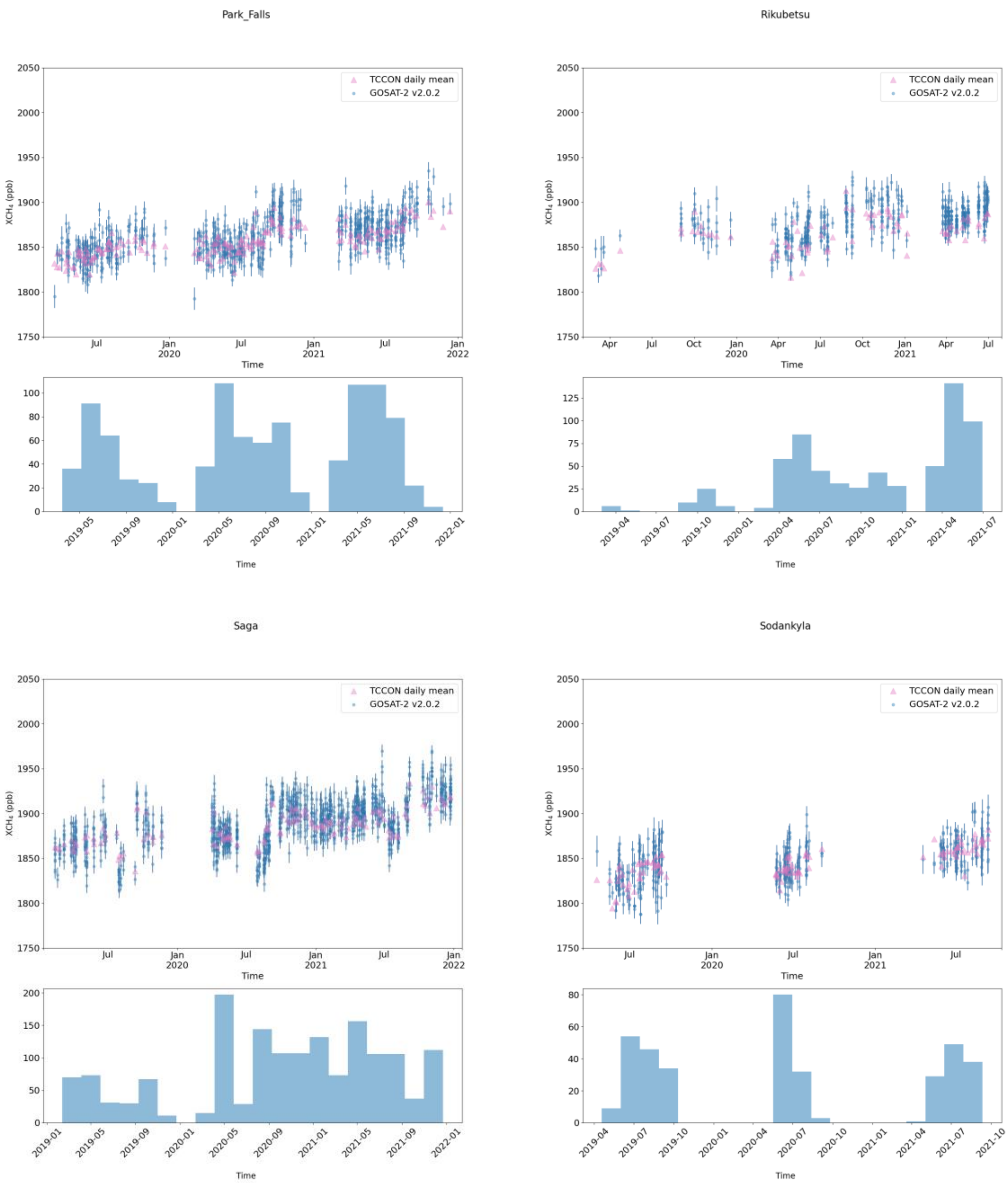

Figure 4.3 Cont.

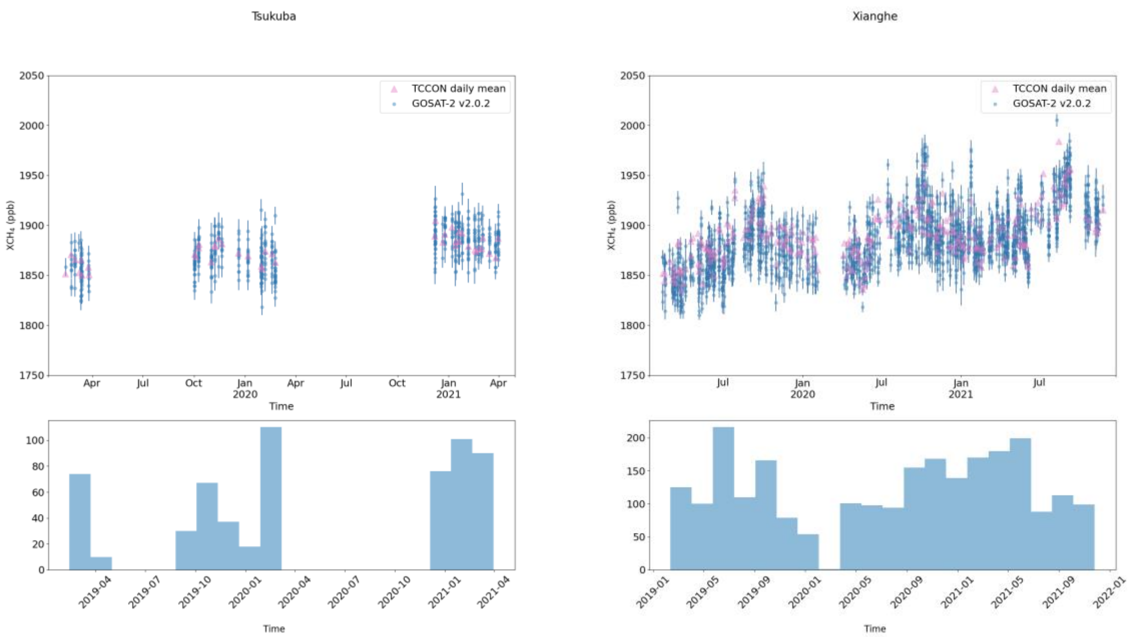

Figure 4.3 Cont.

4.2 Overview GOSAT statistics

Figure 4.4 shows a comparison of GOSAT-2 and GOSAT XCH_4 for the bias corrected product. Table 4.4 shows a summary of the corresponding statistics. The bias-correction of the observations has been performed with TCCON data as described in section 3.2.2. Overall the products compare well with relatively small biases, high correlations and standard deviations smaller than those found in the comparison with TCCON.

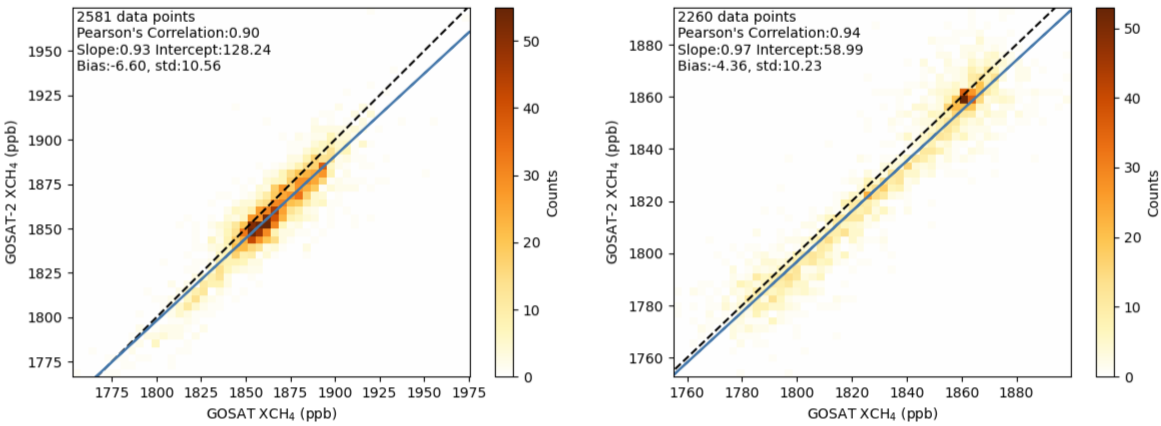

Figure 4.4: Comparison of land (left) and ocean (right) single soundings of XCH_4 with co-located GOSAT and GOSAT-2 measurements for the period Feb2019 - Dec 2021.

Table 4.4. Summary of the comparison of PROXY GOSAT vs GOSAT-2 for daily 2°x2° mean concentrations. Period covered is Feb 2019 to Dec 2021.

Land	N	R	μ (ppb)	σ (ppb)	Ocean	N	R	μ (ppb)	σ (ppb)
	2581	0.90	-6.6	10.6		2260	0.94	-4.4	10.2

4.3 Random error

The error that comes out of the RemoTeC retrieval is just a purely statistical error on the radiance that has been propagated through the entire retrieval chain.

In order to more accurately estimate the actual random error on the GOSAT-2 sounding, we applied the following procedure to obtain a scaling factor with which to scale our statistical error. We take the absolute difference of every co-located sounding and divide it by the retrieved statistical error corresponding to that sounding. We then average these values to obtain the average scaling factor by which to scale the retrieved statistical error to obtain a more correct estimate of the random error.

Based on the analysis, we obtain the following scaling factors for the SRPR XCH_4 product, 1.93 for land mode and 1.66 for glint mode. Subsequently, we calculate the uncertainty ratio which is defined as the ratio of the mean value of the reported uncertainty and the standard deviation of the difference to TCCON. We obtain uncertainty ratios of 0.81 for land mode and 0.81 for glint mode.

The uncertainties in the product are already scaled and represented by the parameter "xch4_uncertainty". The unscaled values are added under the parameter name "raw_xch4_err".

5 Conclusions

This report summarizes the performance of the RemoTeC GOSAT-2 SRPR XCH_4 retrieval. In general, we find very good agreement with TCCON and GOSAT data. All have a very high degree of correlation and show biases and standard deviations similar to the GOSAT SRPR product. The standard deviation of the GOSAT-2 product presented here has improved compared to the SRPR XCH_4 product from C3S v2.0.0 by 4 ppb.

The spatial accuracy (standard deviation site biases) is 5.9 ppb and a single measurement precision of around 16.56 ppb is observed.

6 References

/Barr et al. 2023/ A.G Barr and the GHG-CCI group at SRON: ESA Climate Change Initiative "Plus" (CCI+) ATBD (ATBDv4) for the RemoTeC CH4 GOSAT-2 Data Product CH4_GO2_SRPR v2.0.2 for the Essential Climate Variable (ECV) Greenhouse Gases (GHG), ESA GHG CCI+, 2023.

/Buchwitz et al., 2013/ Buchwitz, M., M. Reuter, O. Schneising, H. Boesch, S. Guerlet, B. Dils, I. Aben, R. Armante, P. Bergamaschi, T. Blumenstock, H. Bovensmann, D. Brunner, B. Buchmann, J. P. Burrows, A. Butz, A. Chédin, F. Chevallier, C. D. Crevoisier, N. M. Deutscher, C. Frankenberg, F. Hase, O. P. Hasekamp, J. Heymann, T. Kaminski, A. Laeng, G. Lichtenberg, M. De Mazière, S. Noël, J. Notholt, J. Orphal, C. Popp, R. Parker, M. Scholze, R. Sussmann, G. P. Stiller, T. Warneke, C. Zehner, A. Bril, D. Crisp, D. W. T. Griffith, A. Kuze, C. O'Dell, S. Oshchepkov, V. Sherlock, H. Suto, P. Wennberg, D. Wunch, T. Yokota, Y. Yoshida, The Greenhouse Gas Climate Change Initiative (GHG-CCI): comparison and quality assessment of near-surface-sensitive satellite-derived CO_2 and CH_4 global data sets, *Remote Sensing of Environment*, doi:10.1016/j.rse.2013.04.024, in press (http://authors.elsevier.com/sd/article/S0034425713003520), 2013.

/**Butz et al., 2011**/ Butz, A., et al.: Toward accurate CO2 and CH4 observations from GOSAT *Geophys. Res. Lett*., 38(L14812), doi:10.1029/2011GL047888, 2011

/**Butz et al., 2009**/ Butz, A., O. P. Hasekamp, C. Frankenberg, and I. Aben: Retrievals of atmospheric CO2 from simulated space-borne measurements of backscattered near-infrared sunlight: accounting for aerosol effects *Appl. Opt*.,48(18), 3322–3322–, 2009

/**Butz et al., 2010**/ Butz, A., O. P. Hasekamp, C. Frankenberg, J. Vidot, and I. Aben, CH4 retrievals from spacebased solar backscatter measurements: performance evaluation against simulated aerosol and cirrus loaded scenes, *J. Geophys. Res*., 115, D24302, doi:10.1029/2010JD014514, 2010

/CECR2017/ R. Detmers, Comprehensive Error Characterisation Report : SRON full-physics retrieval algorithm for XCH4 (SRPR-XCH4) for the Essential Climate Variable (ECV) Greenhouse Gases (GHG) 2017.

/C3SPQAR2019/ L. Wu**,** Product Quality Assessment Report (PQAR) – ANNEX C for products CH4_GOS_SRPR (v2.3.8, 2009-2018) C3S_312a_Lot6_IUP-UC – Greenhouse Gases, 2019.

/Chevalier et al., 2014/ Chevalier, F., Palmer, P.I., Feng, L., Boesch, H., O'Dell, C.W., Bousquet, P., Towards robust and consistent regional CO2 flux estimates from in situ and space-borne measurements of atmospheric CO2, Geophys. Res. Lett., 41, 1065-1070, DOI:10.1002/2013GL058772, 2014

/Chevallier et al., 2019/ Validation report for the CO2 fluxes estimated by atmospheric inversion, v18r2Version 1.0, Copernicus Atmosphere Monitoring Service, ECMWF Copernicus report, CAMS73_2018SC1_D73.1.4.1-2018-v1_201907_Validation inversionCO2fluxes_v1, https://atmosphere.copernicus.eu/sites/default/files/2019-08/CAMS73_2018SC1_D73.1.4.1-2018-v1_201907_v1.pdf

/Krisna et al. 2020/ T. Krisna and the GHG-CCI group at SRON: ESA Climate Change Initiative "Plus" (CCI+) ATBD (ATBDv1.1) for the RemoTeC CH4 GOSAT-2 Data Product CH4_GO2_SRPR for the Essential Climate Variable (ECV) Greenhouse Gases (GHG), ESA GHG CCI+, 2020.

/Laughner et al., 2021/: Laughner, J., Andrews, A., Roche, S., Kiel, M., and Toon, G._ginput v1.0.10: GGG2020 prior profile software (Version 1.0.10), https://doi.org/10.22002/D1.1944, 2021.

/**Schepers et al., 2012**/ Schepers, D., S. Guerlet, A. Butz, J. Landgraf, C. Frankenberg, O. Hasekamp, J.-F. Blavier, N. M. Deutscher, D. W. T. Griffith, F. Hase, E. Kyro, I. Morino, V. Sherlock, R. Sussmann, I. Aben, Methane retrievals from Greenhouse Gases Observing Satellite (GOSAT) shortwave infrared measurements: Performance comparison of proxy and physics retrieval algorithms, *J. Geophys. Res*., 117, D10307, doi:10.1029/2012JD017549, 2012.

/**Toon et al., 2009**/ Toon, G., Blavier, J.F., Washenfelder, R., Wunch, D., Keppel-Aleks, G., Wennberg, P., Connor, B., Sherlock, V., Griffith, D., Deutscher, N., and Notholt, J, Total Carbon Observing Network (TCCON), Optica, JMA3, https://doi.org/10.1364/FTS.2009.JMA3

/Wagner et al., 2012/ Wagner, W., Dorigo, W., de Jeu, R., Parinussa, R., Scarrott, R., Kimmo, Lahoz, W., Doubková, M., Dwyer, N. and Barrett, B.: ESA Soil Moisture CCI: Comprehensive Error Characterisation Report. [online] Available from: http://www.esa-soilmoisture-cci.org/sites/default/files/documents/public/Deliverables%20-%20CCI%20SM%201/20120521_CCI_Soil_Moisture_D1.2.1_CECR_v.0.7.pdf (Accessed 25 January 2016), 2012.

/Wunch et al., 2015/ Wunch, D., Toon, G.C., Sherlock, V., Deutscher, N.M., Liu, X., Feist, D.G., Wennberg, P.O., The Total Carbon Column Observing Network's GGG2014 Data Version. Carbon Dioxide Information Analysis Center, Oak Ridge National Laboratory, Oak Ridge, Tennessee, USA (available at: doi:10.14291/tccon.ggg2014.documentation.R0/1221662), 2015.